Random walks with imperfect trapping in the decoupled-ring approximation

Timo Aspelmeier[1,2], Jérôme Magnin[1,3], Willi Graupner[1,4], and Uwe C. Täuber[1]

[1] Department of Physics, Virginia Polytechnic Institute and State University, Blacksburg, VA 24061-0435, USA
[2] Present address: Department of Physics and Astronomy, University of Manchester, Oxford Road, Manchester M13 9PL, UK
[3] Present address: GeneProt Inc., 2 rue Pré-de-la-Fontaine, CH-1217 Meyrin, Switzerland
[4] Present address: austriamicrosystems AG, A-8141 Schloss Premstätten, Austria

Abstract. We investigate random walks on a lattice with imperfect traps. In one dimension, we perturbatively compute the survival probability by reducing the problem to a particle diffusing on a closed ring containing just one single trap. Numerical simulations reveal this solution, which is exact in the limit of perfect traps, to be remarkably robust with respect to a significant lowering of the trapping probability. We demonstrate that for randomly distributed traps, the long-time asymptotics of our result recovers the known stretched exponential decay. We also study an anisotropic three-dimensional version of our model, where for sufficiently large transverse diffusion the system is described by the mean-field kinetics. We discuss possible applications of some of our findings to the decay of excitons in semiconducting organic polymer materials, and emphasize the crucial influence of the spatial trap distribution on the kinetics.

PACS. 02.50.Ey Stochastic processes. – 05.40.-a Fluctuation phenomena, random processes, noise, and Brownian motion. 05.60.-k Transport processes.

1 Introduction

Random walks in disordered media [1,2] form a class of statistical processes that have been widely employed for the description of an impressive number of physical, chemical and biological phenomena. A particularly interesting subclass is constituted by Brownian motion in the presence of *quenched disorder* in the medium. Depending on the nature of this disorder, significant deviations from the results known for pure random walks are observed. This is true for microscopic quantities (e.g. first passage times, average distance from origin at time t, etc.) as well as for macroscopic properties, such as the asymptotic time evolution of the overall population of random walkers undergoing site-correlated annihilation [1,3].

In the present paper, we address the intermediate and long-time kinetics of random walkers decaying through two simultaneous channels: (i) spontaneous ('radioactive') decay, with no spatial or temporal correlations involved, and (ii) a decay process induced by the presence of non-moving (quenched) imperfect traps in the medium.

In the existing literature, the term 'trap' has been used to describe different types of disorder: In certain instances, the concept of a trap has embodied potential wells in the medium, acting on a walker through delaying its motion (the 'valley model') [1]. In the present context, we refer to traps simply as sites where particles may undergo spontaneous annihilation with a certain (fixed) probability $0 < q \leq 1$.

Random walks with annihilation by trapping have already been the object of considerable attention during the past two decades [4,5,6,7,8,9,10,11,12], to name but a few which are of relevance for this work. These works represent a fundamental and necessary step towards an understanding of transport processes in partially absorbing media. In biology, this applies, e.g., to the scattering of laser light in tissues. In chemistry, microscopic theories of chemical reaction kinetics necessitate to access quantities such as the probability distribution of the nearest-neighbor distance of a diffusing molecule to a (static or moving) trap, representing a reaction center.

In solid-state physics, the study of a whole set of different phenomena in disordered systems relies heavily on the understanding of random walks in the presence of partially absorbing traps: Electron-hole recombination in amorphous solids, and chemical binding by impurities of interstitial hydrogen atoms in metals represent two common examples. More indirectly, this problem is also related to self-attracting polymers, and to the density of states of binary disordered systems, see Ref. [7].

We draw part of our motivation for this present study from a class of organic semiconducting materials which has been the object of considerable attention recently [13]. Due to the nature of their opto-electronic properties, thin

films of organic molecules working as semiconducting diodes [14] are already employed in high-performance electroluminescent displays [15]. For the initial experimental studies of excited states in these materials, aiming at understanding their fundamental properties, light is used for their generation — in most cases the elementary excitations take the form of a bound electron-hole pair [16]. These excitations behave as pseudo-particles (*excitons*) which diffuse and interact in varying and complex ways with the medium [17], and eventually annihilate by emitting photons or phonons. The latter, non-radiative annihilation process is known to be mediated by chemical defects [18].

Experimental studies suggest that the physics of relaxation at work in such excitable media depends in a rather tight and non-trivial way on a variety of partially controllable parameters. Among them, we quote the chemical nature of the material used, the way it has been prepared and/or altered by techniques like photo-oxidation, and the configurational structure at the microscopic level as well as interactions between individual polymer chains. These mutual interactions are markedly different in solid or liquid solutions [19], and amorphous or polycrystalline films, respectively. The detailed relaxation mechanisms, and their dependence on sample properties are as yet incompletely understood, as far as their relation to the elementary and fundamental processes involved are concerned. We believe that the present, somewhat unsatisfactory situation calls for an effort in investigating, e.g., through simple kinetic statistical models, the role played by these different parameters.

In addition, the effectively one-dimensional (or at least strongly directed, anisotropic) nature of exciton transport in organic semiconductors renders simple mean-field theory approaches inadequate. Rather, one expects marked fluctuation and correlation effects. For the model studied here, these in turn should strongly depend on the spatial defect distribution. Thus, experiments probing the exciton kinetics in semiconducting polymers promise to provide an excellent testing ground for a wide variety of non-equilibrium statistical models. Indeed, the dynamics of laser-induced excitons in $N(CH_3)_4MnCl_3$ (TMMC) polymer chains appears to be the best experimental realization to date for diffusion-limited fusion processes $A + A \to A$, where (in an intermediate time window) the predicted power law for the particle density $n \sim t^{-1/2}$ has actually been observed unambiguously [20].

The present paper is organized as follows: In Sec. 2 we provide a precise definition of our model of a random walk with imperfect traps (inducing *non-radiative* exciton recombination) and spontaneous annihilation (or *radiative* recombination). Our main interest being the intermediate and long-time decay of the overall population of particles, the following section presents a calculation of the temporal behavior of this quantity in a one-dimensional setup. It is known that the low dimensionality has a strong impact on the late-time asymptotics of the decay rate [1,3,6]. Our analytical method is based on a scheme that we name the 'decoupled-ring' approximation. Similar approaches have

been used in the literature [10,5]. We demonstrate that the late-time resummation of our analytical result reproduces the known asymptotic, very slow stretched-exponential decay [4,6,8]. Section 4.1 investigates, by means of Monte Carlo simulations, the range of validity for this analytic result when the trapping probability departs from one, the value for which the decoupled-ring approximation becomes exact. In Sec. 4.2, we examine, by way of additional simulations, how the results presented resist to a relaxation of the one-dimensional constraint, by allowing particles to slightly diffuse also in the two transverse directions. Finally, in Sec. 5 we discuss the possibility of applying such a model to account for experimental measurements of exciton decay in organic semiconductors, and comment on the crucial role of the spatial trap distribution for the long-time kinetics.

2 The model

We consider a one-dimensional, regular, infinite lattice $\mathcal{L}$ with linear lattice spacing a. A fraction c of the lattice sites are tagged, thereby denoting that they possess a special property. These particular sites will hereafter be referred to as 'traps', indicating their specific role in the dynamics we are about to introduce.

In general, the spatial trap distribution can be arbitrary. We shall single out two generic, contrasting situations:

1. The trap distribution is *random*, i.e., the distance between two consecutive traps along the chain is represented by a stochastic variable with poissonian distribution.
2. The location of the traps is *spatially correlated*. This case typically covers the situation of n-modal intertrap spacings, or, more generically, situations where some kind of regularity (*order*) can be identified in the way traps are distributed over the system.

Both situations are encountered in experimental samples: If properly synthesized, semiconducting polymer chains in solution may be considered to be essentially trap-free, except for their extremities perhaps, thus falling into the second category. Photo-oxidation of the same material leads to the creation of defects at random locations along the chain, and the first of the two above cases then applies.

We now introduce entities, representing (pseudo- or quasi-)particles, initially randomly distributed over the lattice sites, with density $0 < \rho_0 \leq 1$. A discrete dynamics is implemented, by allowing particles to perform symmetric random walks: A particle located at site k at time t can subsequently be found either at $(k - 1, t + \tau)$ with probability $1/2$, or at $(k + 1, t + \tau)$ with the same probability, where τ denotes the physical timestep associated to the iteration of the dynamics.

At each timestep, every diffusing particle may annihilate through two different decay channels:

– Spontaneous *decay*, occuring with fixed probability $0 \leq p < 1$. For excitons in organic semiconductors, this channel represents *radiative* recombination.

– Stochastic *capture* by a trap: If the diffusing particle enters a tagged site, it annihilates with a given probability $0 < q \leq 1$. For our later application to exciton kinetics, we specify this trap-mediated decay process to be *non-radiative*, i.e., not emitting light at visible wavelengths.

In both cases, the particle is simply removed from the system. The situation with $q = 1$ will be referred to as *perfect traps*.

As both decay process act concurrently without directly influencing each other, their combined effect appears as the product of two *independent* factors. The spontaneous decay being trivially described by a simple exponential relaxation, the real difficulty here rests in the contribution to the kinetics related to the traps, where the dynamical build-up of spatio-temporal correlations renders any mean-field type of approach invalid in (sufficiently) low dimensions. As we shall see, the spatial arrangement of the traps may crucially determine the long-time asymptotics of the particle decay in this situation.

3 Asymptotic kinetics in the decoupled-ring approximation

3.1 Motivations

The model of perfect, uncorrelated traps in one dimension has been solved by Anlauf [9] by means of the span distribution function for one-dimensional random walks. The model of imperfect trapping has been treated in the literature by various means. Weiss and Havlin [10] studied the system in one dimension by introducing a modified model where particles are either destroyed or *reflected* at a trap, thus decoupling the line segments separated by a trap. This calculation was redone and some errors were corrected in [8]. Additionally, the coupled system was mapped to a harmonic chain with random masses and the authors were able to obtain the long-time behaviour of the particle decay in one dimension. We chose a similar approach to [10] by decoupling line segments by cutting the infinite line at each trap and bending each segment onto itself to form a ring (see Fig. 1). The advantage of this method over the approach of mapping to a harmonic system with random masses is that it is easy to obtain results for correlated traps: since each decoupled ring can be treated seperately, the final result is simply obtained by averaging over the ring lengths with the appropriate probability distribution. The disadvantage is that it contains uncontrolled approximations since particles can never leave their ring and wander off into other regions as they could in the original model. However, computer simulations show that these approximations are surprisingly good, in particular for not too low trapping probabilities. For perfect traps, the decoupled model even becomes exact since the traps prevent passage between segments even in the original model.
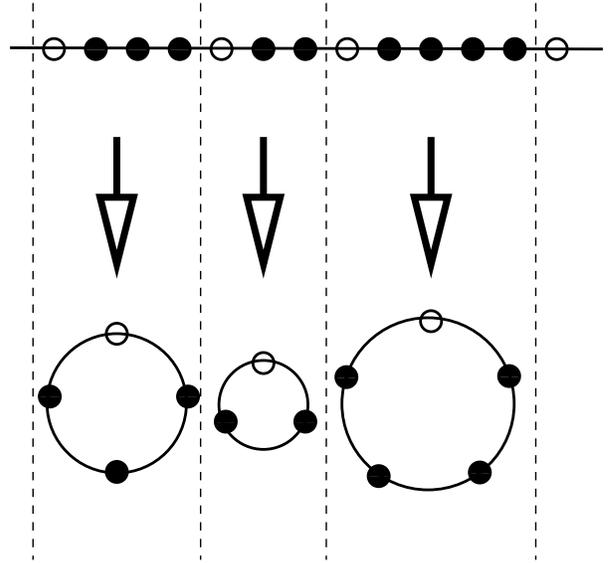
Fig. 1. Schematic illustration of the *ring-decoupling procedure*. Black dots represent regular lattice sites, white ones those with a trap. The infinite, one-dimensional chain is split into segments (delimited by the location of the traps), each of which is then closed onto itself to form a ring. The entire chain is thereby mapped onto an infinite set of rings of varying lengths. This approximation becomes exact in the limit of perfect traps.

3.2 Single-ring solution

Here, we briefly sketch the solution of the model on a single ring of length n. The discrete time dynamics takes the form of a master equation for the particle density distribution vector $\boldsymbol{\rho}(t) \equiv (\rho_1(t), \ldots, \rho_n(t))$, with the trap located at site 1 without loss of generality,

$$
\begin{pmatrix} \rho_1 \\ \rho_2 \\ \vdots \\ \rho_{n-1} \\ \rho_n \end{pmatrix}(t+\tau) = \begin{pmatrix} 0 & \frac{1}{2} & 0 & \cdots & 0 & \frac{1}{2} \\ \frac{1-q}{2} & 0 & \frac{1}{2} & & & 0 \\ 0 & \frac{1}{2} & & & & \vdots \\ \vdots & & & \ddots & & 0 \\ 0 & & & & & \frac{1}{2} \\ \frac{1-q}{2} & 0 & \cdots & 0 & \frac{1}{2} & 0 \end{pmatrix} \begin{pmatrix} \rho_1 \\ \rho_2 \\ \vdots \\ \rho_{n-1} \\ \rho_n \end{pmatrix}(t).
$$

(1)

For late times, the overall decay rate of the concentration is 'slaved' to the largest eigenvalue α_n of the above matrix, and its corresponding eigenvector $\boldsymbol{a}$. The calculation is straightforward and is shown in App. A.1; the result is

$$\alpha_n = \cos \phi_n, \text{ where} \tag{2}$$

$$\phi_n = \frac{\pi}{n} - \frac{2\pi(1-q)}{q}\frac{1}{n^2} + \frac{4\pi(1-q)^2}{q^2}\frac{1}{n^3} + \mathcal{O}(n^{-4}) \tag{3}$$

for the eigenvalue and

$$a_1 = 1, \tag{4}$$

$$a_k = \cos(k-1)\phi_n + q\frac{\sin(k-2)\phi_n}{\sin \phi_n} \tag{5}$$

for the eigenvector.

Starting from an initial distribution $\rho_k(t = 0)$, the long-time solution is

$$\boldsymbol{\rho}(t) \overset{t,n\to\infty}{\sim} \frac{(\boldsymbol{a}, \boldsymbol{\rho}(0))}{(\boldsymbol{a}, \boldsymbol{a})} \, \boldsymbol{a} \, e^{t \ln \alpha_n}, \qquad (6)$$

where $(\cdot, \cdot)$ denotes the scalar product. The scalar products can be worked out for a homogeneous initial distribution, $\rho_k(0) = \rho_0$, to leading order in $1/n$, and the result for the mean density on the ring $\overline{\rho}$ is

$$\overline{\rho}(t) \equiv \frac{1}{n} \sum_{k=1}^n \rho_k(t) \overset{t,n\to\infty}{\sim} \frac{8}{\pi^2} \rho_0 \, e^{t \ln \alpha_n}. \qquad (7)$$

Note that this result is better than might be expected at first sight because the overlap of the eigenvector $\boldsymbol{a}$ with the initial homogeneous configuration is very large (see App. A.1),

$$\frac{(\boldsymbol{a}, \boldsymbol{\rho}(0))}{|\boldsymbol{a}||\boldsymbol{\rho}(0)|} = \frac{2\sqrt{2}}{\pi} + \mathcal{O}(1/n) \approx 0.9\ldots, \qquad (8)$$

which guarantees that this result is good even at intermediate times.

3.3 Full-chain solution

Given an *arbitrary* distribution of traps, one can now write down the solution for the full chain (in the decoupled-ring approximation) by simply superposing the single-ring results, properly weighted with the relative abundance for the occurrence of rings of length n in the chain. For example, if there are well-defined trap spacings such that only a *finite* number of certain values of $n_i, i = 1, \ldots, k$ is possible, with relative abundance $P(n_i)$, then the final result is simply a sum of k terms of the form (7), each multiplied with $P(n_i)$. As is evident from Eq. (7), the terms for large n will quickly dominate, and the maximum value $n_{\max}$ will govern the long-time limit.

For a random (poissonian) initial distribution of the traps with concentration $0 < c < 1$, all values of n are possible, the probability of finding a ring of size n being given by

$$P(n) = nc^2(1 - c)^{n-1} \, . \qquad (9)$$

This allows us to finally write

$$\overline{\rho}(t) \overset{t\to\infty}{\sim} \frac{8}{\pi^2} \rho_0 \, c^2 \sum_{n=1}^{\infty} n(1 - c)^{n-1} \times \qquad (10)$$

$$\times \exp\left[t \ln \cos\left(\frac{\pi}{n} - \frac{2\pi(1-q)}{q}\frac{1}{n^2} + \frac{4\pi(1-q)^2}{q^2}\frac{1}{n^3}\right)\right].$$

For $t \to \infty$, the late-time asymptotics of the *infinite* sum (10) can be extracted (see the appendix). The result reads:

$$\overline{\rho}(t) \overset{t\to\infty}{\sim} \rho_0 \frac{8}{-\ln(1-c)} \frac{c^2}{1-c} \sqrt{\frac{2}{3\pi}} t^{1/2} \times$$

$$\times \exp\left[-\frac{2(1-q)}{q} \ln(1-c)\right] \times$$

$$\times \exp\left[-\frac{3}{2}[-\pi \ln(1-c)]^{2/3} t^{1/3}\right] . \qquad (11)$$

We recover the known *stretched exponential* long-time decay [6,8,9] $\overline{\rho}(t) \sim \exp(-\text{const.} \, t^{1/3})$ with the correct values for both the exponent and its prefactor, and including a q-dependent enhancement factor in agreement with [8] (higher order correction terms have been omitted here for brevity). With a *random* (Poissonian) distribution of traps, one therefore expects a much *slower* asymptotic time decay than for a typical correlated distribution. Certainly, for any finite number of allowed values of n, the asymptotic temporal decay will be a simple exponential. As another example, a Gaussian distribution of the lengths of trap-free regions (around some mean value) leads to a stretched exponential with exponent $1/2$ (by a calculation analogous to the one above). Thus, in addition to the trap concentration and the induced decay probability q, the spatial arrangement of the traps is of crucial importance.

Instead of using the asymptotic result Eq. (11) we prefer to use Eq. (10) (suitably truncating the sum) for our comparisons with simulations and experiments below since it applies not only to the long times but also to intermediate times. This is essential as it is known that the crossover to the long-time behaviour Eq. (11) may set in so late to be unreachable in practice (see e.g. [11] and references therein, [7,12]).

4 Monte Carlo simulations

4.1 Strictly one-dimensional system

We have investigated the range of validity of the result (10) emerging from our decoupled-ring approximation by means of Monte Carlo (MC) simulations. The parameter of interest is of course q, the trapping probability. For q equal (or very close) to 1, Eq. (10) should perform very well. This agreement may be expected to degrade when q is lowered significantly below unity, since this implies an increasing coupling between adjacent rings that has been completely neglected in our treatment of the problem.

Figure 2 shows a set of plots comparing results of MC simulations to the approximate analytic formula (10), for different values of the trapping probability q. The spatial trap distribution is random (poissonian). For clarity, we have set the spontaneous decay probability p to zero here. No crossover may anyway be expected between the exponential and stretched exponential components of the dynamics: Due to the structure of Eq. (11), the sub-exponential behavior is screened out by the spontaneous
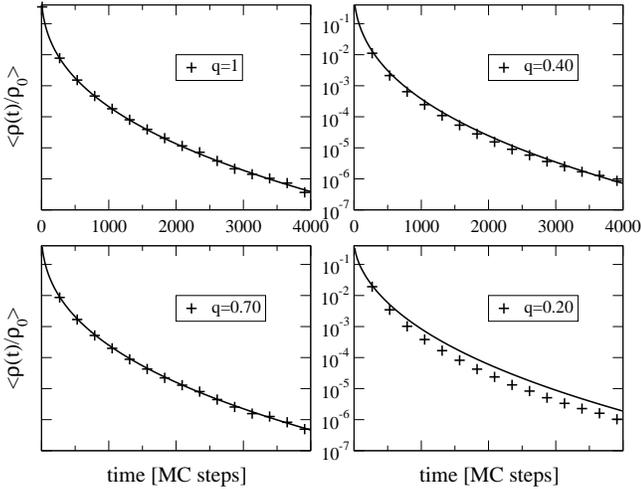
Fig. 2. Monte Carlo simulations for the one-dimensional imperfect trapping process. The dimensionless quantity on the vertical axis is the amount of random walkers present in the system, normalized by the initial total population. It can also be interpreted in a statistical sense, as the survival probability of a *single* walker. Crosses represent the numerical result, averaged over ~ 5000 independent runs. The solid lines represent the analytical result of the ring-decoupling scheme, as given by Eq. (10). The following choice of parameters was made: system size$=2^{14} = 16384$ sites; p (spontaneous decay probability) $= 0$; c (trap concentration) $= 0.2$; diffusion coefficient $= 0.5 \, [a^2/\tau]$; ρ_0 (initial particle density) $= 0.6$.

Fig. 3. Monte Carlo simulations for the one-dimensional imperfect trapping process with fixed trapping probability and varying traps concentration. The quantities on the axis and the meaning of the symbols chosen are the same as for figure 2. Results have been averaged over ~ 5000 independent runs. The following choice of parameters was made: system size $= 2^{14} = 16384$ sites; p (spontaneous decay probability) $= 0$; q (trapping probability) $= 0.4$; diffusion coefficient $= 0.5 \, [a^2/\tau]$; ρ_0 (initial particle density) $= 0.6$.
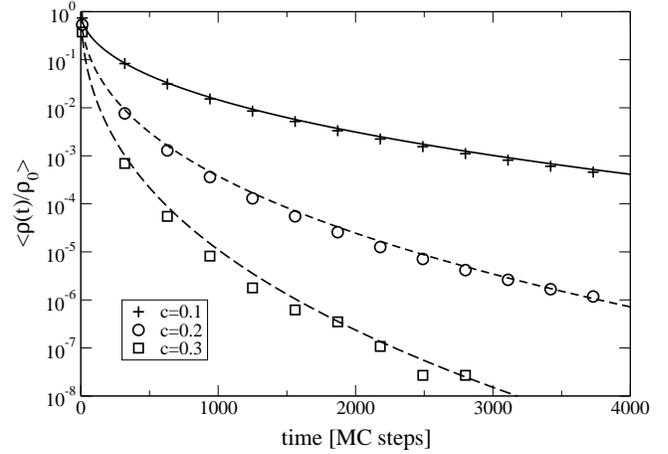
exponential decay for all real and positive values of the time t.

The first (upper left) graph for $q = 1$ serves as a reference for a visual evaluation of the uncertainty in our numerical data. Looking at the other graphs in the figure, one observes that for the chosen trap concentration ($c = 0.2$), the analytical result performs remarkably well down to $q \cong 0.4$ (!). Note that the finiteness of the systems simulated implies a temporal horizon: Beyond this limit, both strong depletion in particles and inaccurate statistics for large, trap-free regions (which play an increasingly important role for late times) conspire to render the simulation meaningless. Our approximation being an asymptotic theory, there is however no doubt that the matching between Eq. (10) and the numerical data is at least as good for the unexplored, late time domain as it appears in the 'early-time' regime depicted in Fig. 2.

Figure 3 illustrates how the decoupled-ring approximation performs upon varying the trap concentration at fixed trapping probability.

4.2 Anisotropic three-dimensional system

Semiconducting polymer chains can be found in various configurations: When in solution, they can be considered as totally isolated from each other, hence representing a set of one-dimensional segments on which excitons propagate and interact. They can, however, also be organized in

a more cohesive manner, namely in the form of a network characterized by a certain degree of coupling between the polymer chains, or even in highly ordered structures such as polycrystalline films. This interaction between chains is evident both in the chain-to-chain transfer of charges when these networks are used in light emitting diodes, as well as in the chain-to-chain transfer of excitons [22]. In these cases, the one-dimensional character of the exciton dynamics is likely to be broken, the 'particles' being able to 'cross-diffuse' from one chain to a neighboring one.

In this context, an interesting question that naturally arises is the following: To which extent does the picture related to the ideally one-dimensional case break down, once a small degree of cross-diffusion is allowed in a set of one-dimensional chains forming a crystal-like structure? For we know that in an isotropic three-dimensional system with uncorrelated traps, the long-time behaviour of the system is given by a stretched exponential of the form $\rho(t) \sim \exp(-\text{const.}\, t^{3/5})$ [4,6].

Our one-dimensional model is extended to three dimensions by allowing particles to hop in all three spatial directions, but with different rates. In particular, we single out one direction as the direction of the polymer chains and allow hopping along this direction as in the one-dimensional model with a diffusion constant D_l. Transverse hopping is suppressed by choosing a transverse diffusion constant $D_t < D_l$. Thus, a particle hops along the polymer direction with probability $P_l = (2D_t/D_l + 1)^{-1}$ and perpendicular to it with probability $1 - P_l$ at each time step.

Figure 4 displays the result of MC simulations of our model in three dimensions, where the ratio of the trans-
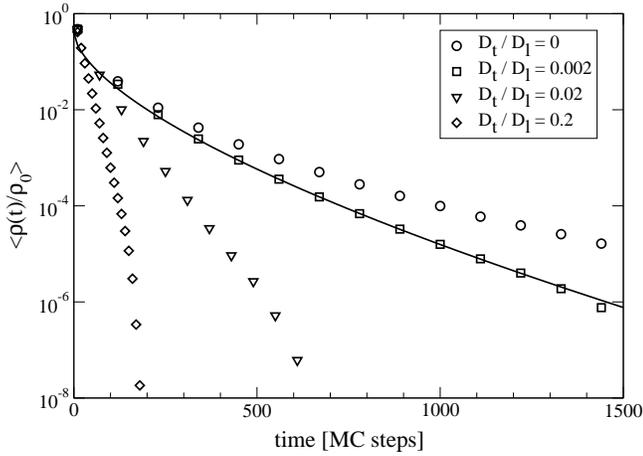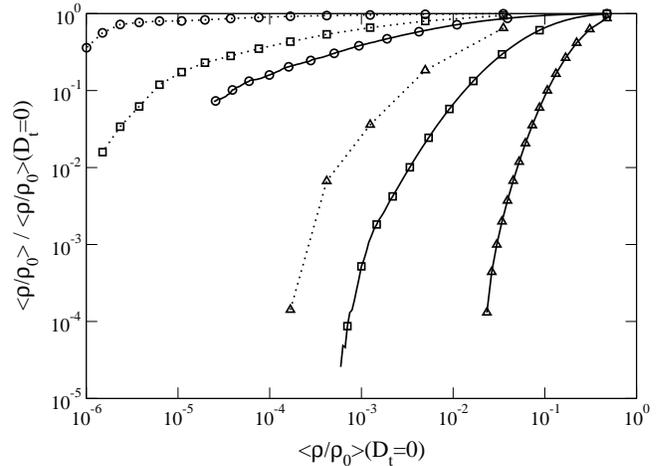
Fig. 4. Monte Carlo simulations of a three-dimensional imperfect trapping process competing with spontaneous decay (see the caption of Fig. 2 for comments on the axis and units). Symbols represent the numerical results for different values of the transverse diffusion coefficient D_t, as indicated in the legend. They have been averaged over ca. 100 runs. The solid line shows a fit with a stretched exponential $\exp(-at^{3/5})$ as appropriate for a truly three-dimensional system, showing that at $D_t/D_l = 0.002$ and $c = 0.2$ the system already behaves like a three-dimensional one. The following choice of parameters was made: system size $= 2^{12} \times 2^5 \times 2^5$ sites; $p = 0.001$; $c = 0.2$; $q = 0.5$; longitudinal diffusion coefficient $D_l = 0.5$ $[a^2/\tau]$; $\rho_0 = 0.6$.


Fig. 5. Effect of the trap concentration on the relaxation of the one-dimensional constraint. The same simulations as in Fig. 4 were performed for a higher trap concentration $c = 0.7$ (averaged over ~ 100 runs here, too), and both sets are now displayed together. Solid lines correspond to $c = 0.2$, and dotted ones to $c = 0.7$. For each of the three cases with $D_t \neq 0$, the plot shows the *relative* deviation from the $D_t = 0$ case. Circles, squares, and triangles indicate respectively the simulations with values $D_t/D_l = 0.002, 0.02$, and 0.2.

verse and longitudinal diffusion rates D_t/D_l has been chosen non-zero, but kept small. The virtue of this figure is to undoubtedly show the extent to which the topology affects the dynamics in this process: Even a very small relaxation of the one-dimensional constraint results in a drastic effect. This is easily understood if one takes into consideration the two following important aspects of the dynamics:

- The increasing role played by trap-free regions of larger and larger size as time increases.
- The fact that a particle jumping transversely onto a neighboring chain has, statistically, large chances to penetrate a small inter-trap segment, and therefore decay rapidly. This is of course true only under the hypothesis that the trap distributions for all chains are totally uncorrelated with respect to each other.

On the other hand, we see that the decoupled-ring approximation, which correctly captures only the one-dimensional topology, numerically remains a fairly adequate description for small anisotropy ratios.

In Fig. 5, we examine how the trap concentration affects the amplitude of the effect of the relaxation of the one-dimensional constraint on the population decay. As shown, a higher trap concentration helps to screen out the emergence of the transverse channel for diffusion. This is an important observation when one tries to use our model to interpret experimental data, as we will see in the forthcoming section.

# 5 Applicability to the decay of excitons in quasi-one-dimensional organic semiconductors

As previously mentioned, our model may be considered a potential candidate for a 'minimal' description of the decay dynamics of excitons in organic semiconductors. Confrontation with real data coming from experimental measurements of such a decay is therefore instructive. The figures below display our attempts to fit such experimental data with our analytical result (10), supplemented with a spontaneous decay factor e^{-pt}.

The data presented here, orginally reported in Ref. [23], measure (in frequency space) the response of ladder-type Poly(*Para*-Phenylene) (LPPP) to excitation by a modulated light beam. The signal represents the Fourier transform of the spectrally integrated photoluminescent emission of the material. This is given by the *activity*, i.e., the number of *radiative* recombinations of excited electronic states (excitons) per time interval. Thus, while both spontaneous and trap-induced decay channels reduce the exciton population, only the activity due to the spontaneous radiative recombination is monitored by the data. Three different types of samples, all made from the same material, were analyzed: The polymer in solution, a pristine polymer film, and the same film after it had been subjected to photooxidization. In the following, we report our comparison of theoretical and experimental data for each case.

Figures 6–8 show the experimental data as real and imaginary parts. The solid lines are simultaneous fits (performed with a Levenberg-Marquardt algorithm) to both
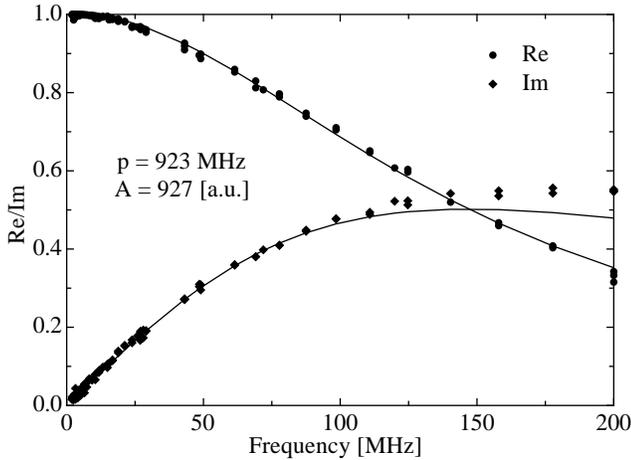
Fig. 6. Fourier transform of the response function as measured (dots) and a fit (solid lines) with the Fourier transform of the activity for an exponential time decay for the polymer in solution. Fit parameters are the spontaneous decay rate p and an (irrelevant) overall amplitude A, given in arbitrary units.
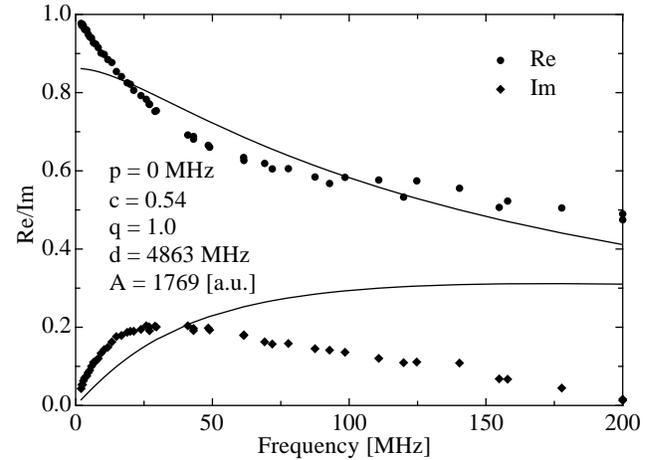
Fig. 8. Fourier transform of the response function as measured (dots) and a fit (solid lines) with the Fourier transform of the activity corresponding to the time decay according to Eq. (10) for the non-oxidized film. Fit parameters are as in Fig. 7. The agreement is very poor, see text.
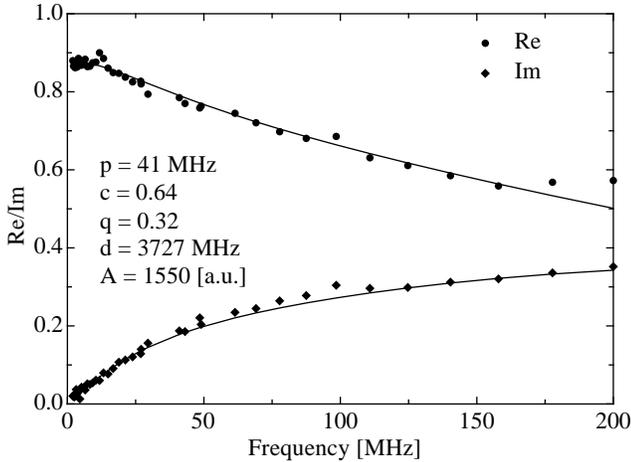
Fig. 7. Fourier transform of the response function as measured (dots) and a fit (solid lines) with the Fourier transform of the activity corresponding to the time decay according to Eq. (10) for the photo-oxidized film. Fit parameters are the spontaneous decay rate p, the trap concentration c, the trapping probability q, the exciton hopping rate d, and an (irrelevant) overall amplitude A. The agreement is quite satisfactory.

real and imaginary parts with a Fourier transform of the activity corresponding to a single exponential in the case of the solution, Fig. 6, and to a decay following Eq. (10) in the case of the photo-oxidized and non-odixized films, respectively, Figs. 7 and 8.

For the solution, Fig. 6, the experimental data can very well be described by a single exponential (Lorentzian in Fourier space). The polymer chains have very few defects, apart perhaps from their end-points which may act as traps, and have all the same lengths — this results in an almost purely exponential decay of the exciton population since the lengths of the trap-free regions are monodisperse (in the sense of the decoupled-ring approximation).

For the oxidized film, Fig. 7, the situation changes entirely. First, when going from solution to film we introduce a coupling between the chains which is *not* present in the solution. Second, due to oxidization, many defects acting as traps have been introduced on the film, see Ref. [23](b). Accordingly, Eq. (10) describes the data well, even though it has been devised for one-dimensional systems rather than films. This may be explained by the large number of traps (around 65% of the *effective* sites according to the fit), which prevent the excitons from 'feeling' the three-dimensional nature of the film, as Fig. 5 clearly illustrated in the preceding section. Further support for this effective confinement of excitons to a single chain and the high number of traps is given in Ref. [23](b), based on an analysis of the emission and absorption photoluminescence spectra.

There are, of course, errors in the values of the fit parameters. The greatest uncertainty comes from the spontaneous decay rate p, which induces very large errorbars on all other parameters as well (not shown in the figures). If, however, p is kept fixed at the value indicated in Fig. 7 and only the remaining parameters are used for fitting, the error in e.g. the trap concentration is found to be about 15%. Nevertheless it should be kept in mind that our most important result here is the functional form of our theoretical curve which is able to reproduce the data rather than precise values of the parameters.

The observed photoluminescence decay-time has been greatly *increased* compared to the solution, in spite of the presence of traps. At the same time we know that the major decay path for this sample is non-radiative because the photoluminescence quantum yield is only a few percent. Hence, the long-living photoluminescence must be the signature of a 'stabilized species' which is *not* photogenerated with a high yield. This may be due to low-energy sites on the polymers which capture the excitons and prevent them from decaying spontaneously, or delayed photolumi-

nescence due to triplet-triplet annihilation. Evidence for the latter process in this particular material can be found in Ref. [24]. Neither of these processes have been included in our simplified model.

Turning to the last of the three sets of data, the non-oxidized film shown in Fig. 8, we observe that it can neither be described by a single exponential nor with Eq. (10). Fig. 8 shows the result of an unsuccessful fitting attempt with Eq. (10). Apparently, the influence of the three-dimensional nature of the film made from the *same* molecules as were measured in solution first, cannot be described simply by the introduction of traps. Accordingly, since our model is not appropriate for the non-oxidized film, the actual values of the fit parameters as shown in Fig. 8 are entirely meaningless.

This has an important implication. The non-oxidized film has a photoluminescence quantum yield of 30% vs. nearly 100% for the solution of the same molecules. One way to account for this could be the formation of traps during the film forming process, e.g. by conformational stress on the molecules [25]. If this was the case, our model would capture this effect and describe it properly. Hence, the reduction of the quantum yield and the difference in photoluminescence dynamics between film and solution have to originate from a *different* solid state effect.

6 Summary and conclusion

We have considered a model of random walkers undergoing decay through both capture by imperfect traps *and* spontaneous decay. In one dimension, we have derived an explicit analytical form for the time dependence of the survival probability, based on the ring-decoupling approximation scheme, supplemented with an asymptotic expansion. We have demonstrated that this result, although exact only in the limit of perfect traps, performs remarkably well upon lowering of the trapping probability when confronted to numerical simulations. Extension of our simulations to three dimensions, albeit with anisotropic diffusion, have illustrated the high sensitivity of the decay rate to the low-dimensionality constraint.

An application of our findings to the understanding of the decay dynamics of excitons in semiconducting polymers has been attempted. We conclude that within our model traps alone cannot account for the observed difference between exciton dynamics in a pristine solution and film made from the same conjugated polymer, LPPP. Photo-oxidizing LPPP leads to isolated segments which probably correspond to the one-dimensional case in our model. The large concentration of effective trap sites obviously dominates over all other physically relevant mechanisms.

In this context, it is important to emphasize again the crucial role played by the *spatial* trap distribution. For a more or less regular spacing of defects, the long-time kinetics would be governed by a simple exponential, with a 'renormalized' decay rate. For a random trap distribution, on the other hand, a much slower stretched exponential decay ensues asymptotically. At least in the long-time limit, one might therefore quite drastically control the exciton population through appropriate 'engineering' of the spatial arrangement of the trapping defects.

At any rate, our model system demonstrates again the importance of including statistical fluctuations effects effectively low-dimensional samples. This is of course a well-established fact in statistical mechanics model systems. Yet to date there have been few examples where clear evidence of correlations not captured by mean-field theory has been found in real experiments on non-equilibrium systems. Moreover, we believe that our study underscores the relevance of simplified kinetic models, at least in the long-time limit, where detailed microscopic mechanism become less prominent. We hope that a better understanding of, e.g., the important organic semiconducting materials will eventually be achieved through combining experimental data with both quantum-mechanical computations and more macroscopic, statistical approaches.

A Appendix: Decoupled-ring approximation

A.1 Computation of eigenvectors and eigenvalues

In this appendix, we show how to compute the *symmetric* eigenvectors and eigenvalues of the matrix

$$
M = \begin{pmatrix}
0 & \frac{1}{2} & 0 & \cdots & 0 & \frac{1}{2} \\
\frac{1-q}{2} & 0 & \frac{1}{2} & & & 0 \\
0 & \frac{1}{2} & & & & \vdots \\
\vdots & & & \ddots & & 0 \\
0 & & & & & \frac{1}{2} \\
\frac{1-q}{2} & 0 & \cdots & 0 & \frac{1}{2} & 0
\end{pmatrix}
\tag{12}
$$

appearing in Eq. (1). The anti-symmetric eigenvectors, also present in principle, are irrelevant in this context because they have vanishing overlap with the initial homogeneous particle distribution. We therefore try a symmetric

ansatz of the form

$$
\mathbf{a} \equiv \begin{pmatrix} 1 \\ a_2 \equiv \alpha \\ a_3 \\ a_4 \\ \vdots \\ a_{n-2} = a_4 \\ a_{n-1} = a_3 \\ a_n = a_2 = \alpha \end{pmatrix} , \tag{13}
$$

and note that this implies $(M\mathbf{a})_1 = \alpha$ which identifies α as the prospective eigenvalue corresponding to $\mathbf{a}$. We can then read off that the second component of $M\mathbf{a}$ is given by

$$
(M\mathbf{a})_2 = \frac{1-q}{2}a_1 + \frac{1}{2}a_3 , \tag{14}
$$

which must be equal to αa_2 since $\mathbf{a}$ is supposed to be an eigenvector. This gives

$$
a_3 = 2\alpha^2 - 1 + q . \tag{15}
$$

By a similar argument, the following recursion relation can be derived for the other entries of the eigenvector:

$$
a_k = 2\alpha a_{k-1} - a_{k-2} \quad (k \geq 4) . \tag{16}
$$

This kind of second-order recursion relation has two exponential solutions $r_\pm^{k-2}$ (the -2 in the exponent is for later convenience), and a_k is given by a linear superposition of them, $a_k = A r_+^{k-2} + B r_-^{k-2}$. Plugging the ansatz r^{k-2} into the recursion relation Eq. (16) yields a quadratic equation for r with the two solutions $r_\pm = \alpha \pm i\sqrt{1-\alpha^2}$. Noting that $0 \leq \alpha < 1$ is implied by the non-conserved number of particles owing to the trap and the fact that the particle density cannot be negative, this can be written in terms of an angle ϕ with $\alpha = \cos\phi$ as $r_\pm = e^{\pm i\phi}$.

The initial conditions $a_2 = \alpha$ and $a_3 = 2\alpha^2 - 1 + q$ now determine the constants A and B; a straightforward calculation gives

$$
A = B^* = \frac{1}{2}e^{i\phi} + \frac{q}{e^{i\phi} - e^{-i\phi}} , \tag{17}
$$

resulting in

$$
a_1 = 1 ,
$$
$$
a_k = \cos(k-1)\phi + q\frac{\sin(k-2)\phi}{\sin\phi} \quad (2 \leq k \leq n) . \tag{18}
$$

It now only remains to be checked that $a_n = a_2$, as imposed from the beginning. This condition determines ϕ and, after some algebra, results in the following equation:

$$
[1 - (1-2q)\cos 2\phi]\sin n\phi
$$
$$
-[1 - (1-2q)\cos n\phi]\sin 2\phi = 0 . \tag{19}
$$

The smallest non-zero solution to this equation leads to the sought-for largest eigenvalue $\alpha = \cos\phi$ [even though

$\phi = 0$ is technically a solution to Eq. (19), it is not a valid one since the constant A does not exist for $\phi = 0$]. Assuming that the smallest ϕ can be represented by a perturbative expansion as $\phi = \frac{c_1}{n} + \frac{c_2}{n^2} + \cdots$, Eq. (19) can be expanded in powers of $1/n$ and the coefficients c_i are readily evaluated. The result is

$$
\phi = \frac{\pi}{n} - 2\pi\frac{1-q}{qn^2} + 4\pi\frac{(1-q)^2}{q^2 n^3} + \mathcal{O}(n^{-4}) . \tag{20}
$$

Overlap of the eigenvectors with the initial state

As seen in Sec. 3, we also need to know the overlap of the eigenvector found in the preceding subsection with the initial homogeneous particle distribution, i.e., we need to calculate

$$
(\mathbf{a}, \mathbf{1}) = \sum_{k=1}^{n} a_k , \quad \text{and} \quad (\mathbf{a}, \mathbf{a}) = \sum_{k=1}^{n} a_k^2 . \tag{21}
$$

The symbol $\mathbf{1}$ here stands for the vector with all entries equal to 1. Both sums can be evaluated tediously but straightforwardly by inserting Eq. (18) and noting that both of them can be written in terms of geometric series. The resulting expression may be evaluated further for large n by inserting $\phi = \pi/n + \mathcal{O}(n^{-2})$. The results read

$$
(\mathbf{a}, \mathbf{1}) \overset{n\to\infty}{\sim} \frac{2qn^2}{\pi^2} , \quad \text{and} \quad (\mathbf{a}, \mathbf{a}) \overset{n\to\infty}{=} \frac{q^2 n^3}{2\pi^2} . \tag{22}
$$

Altogether this gives

$$
\frac{(\mathbf{a}, \mathbf{1})^2}{(\mathbf{a}, \mathbf{a})} \overset{n\to\infty}{\sim} \frac{8n}{\pi^2} . \tag{23}
$$

A.2 Asymptotic evaluation of the long-time behavior

Eq. (10), the main result of this calculation, can be evaluated asymptotically for long times. Since $\phi = \mathcal{O}(1/n)$, the long-time behavior is dominated by the large-n terms in the sum. Using $\alpha = \cos(\phi) = 1 - \pi^2/2n^2 + 2\pi^2(1-q)/qn^3 + \mathcal{O}(n^{-4})$ and ignoring irrelevant prefactors for the moment, Eq. (10) can be written as

$$
\overline{\rho}(t) \propto \sum_{n=1}^{\infty} n \exp\left[n\ln(1-c) - \frac{\pi^2}{2n^2}t + \frac{2\pi^2(1-q)}{qn^3}t \right] . \tag{24}
$$

By introducing $x \equiv t^{1/3}$, the sum on the r.h.s. can be recast as a Riemannian sum approximating an integral in the variable $z = n/x$,

$$
\overline{\rho}(t) \propto x^2 \sum_{n=1}^{\infty} \frac{1}{x}\frac{n}{x} e^{\frac{x^3}{n^3}\frac{2\pi^2(1-q)}{q}} e^{x[n\ln(1-c)/x - \frac{\pi^2 x^2}{2n^2}]} \tag{25}
$$

$$
\overset{x\to\infty}{\sim} x^2 \int_0^\infty dz\, z e^{2\pi^2(1-q)/z^3 q} e^{x[z\ln(1-c) - \pi^2/2z^2]} \tag{26}
$$

This integral may now be evaluated asymptotically by Laplace's method and finally yields, including all prefactors, Eq. (11).

References

1. J.W. Haus and K.W. Kehr, Phys. Rep. **150**, 263 (1987).
2. J.-P. Bouchaud and A. Georges, Phys. Rep. **195**, 127 (1990).
3. Barry D. Hugues, *Random walks and random environments*, vol. 1 (Oxford Science Publ., 1995).
4. B.Ya. Balagurov and V.G. Vaks, Sov. Phys.-JETP **38**, 968 (1974).
5. C. Domb *et al.*, Phys. Rev. **115**, 18 (1959).
6. M. Donsker and S. Varadhan, Commun. Pure Appl. Math. **28**, 525 (1975).
7. Th. M. Nieuwenhuizen, Phys. Rev. Lett. **62**, 357 (1989).
8. Th. M. Nieuwenhuizen and H. Brand, J. Stat. Phys. **59**, 53 (1990).
9. J.K. Anlauf, Phys. Rev. Lett. **52**, 1845 (1984).
10. G.H. Weiss and S. Havlin, J. Chem. Phys. **83**, 5670 (1985).
11. G.T. Barkema *et al.*, Phys. Rev. Lett. **87**, 170601 (2001).
12. L.K. Gallos and P. Argyrakis, Phys. Rev. E **64**, 051111 (2001).
13. J.H. Schoen *et al.*, Science **289**, 599 (2000).
14. R. Friend *et al.*, Physics World, June 1999, pp. 35-40.
15. For an up-to-date compilation, see refs. in *SPIE Proceedings* **4105**, (2001).
16. *Primary Photoexcitations in Conjugated Polymers: Molecular Exciton versus Semiconductor Band Model*, N.S. Sariciftci (ed.), (World Scientific Publ., Singapore, 1997).
17. M. Scheidler *et al.*, Phys. Rev. B **54**, 5536 (1996).
18. M. Yan *et al.*, Phys. Rev. Lett. **73**, 744 (1994).
19. M. Yan *et al.*, Phys. Rev. Lett. **75**, 1992 (1995).
20. K. Kroon, H. Fleurent, and R. Sprik, Phys. Rev. E **47**, 2462 (1993).
21. E.J.W. List *et al.*, Chem. Phys. Lett. **325**, 132 (2000).
22. J.J.M. Halls *et al.*, Appl. Phys. Lett. **68**, 3120 (1996).
23. (a) M. Wohlgenannt *et al.*, Chem. Phys. **227**, 99 (1998); (b) W. Graupner *et al.*, *Materials Research Society Symposium Proc.* **488**, 789 (1998).
24. Y. V. Romanovskii and H. Baessler, Chem. Phys. Lett. **326**, 51 (2000).
25. T.Q. Nguyen *et al.*, J. Phys. Chem. B **104**, 237 (2000).